JOURNAL OF APPLIED ELECTROCHEMISTRY **29** (1999) 321–330.

Tool design in electrochemical machining considering the effect of thermal-fluid properties

C. S. CHANG, L. W. HOURNG, C. T. CHUNG

Department of Mechanical Engineering, National Central University, Chung-Li, Taiwan 32054

Received 12 September 1997; accepted in revised form 7 May 1998

The effect of thermal-fluid properties are considered in the numerical simulation of the tool shape for a given workpiece shape in electrochemical machining. An embedding method is used for this inverse problem. A bubbly two-phase, one-dimensional flow model and a one-phase, two-dimensional flow model are applied to predict the fluid field of the electrolyte, respectively. Results show that the void fraction is the most important factor in determining the electrolyte conductivity and the shape of the workpiece. The proper machining conditions and numerical parameters are important to obtain a good solution. The relative error can be reduced under 0.002.

Keywords: *ECM*, *inverse problem*, *numerical*, *thermal-fluid properties*

List of symbols

A	cross-sectional area (m^2)
C_f	specific heat of electrolyte ($J\,kg^{-1}\,K^{-1}$)
$\vec{E}$	electrical intensity ($V\,m^{-1}$)
f_r	feed rate of the tool ($m\,s^{-1}$)
$f(x)$	given tool shape
g	electrode gap (m)
g_e	equilibrium gap thickness at inlet (m)
H	convective heat transfer coefficient ($W\,m^{-2}\,K^{-1}$)
h	specific enthalpy ($J\,kg^{-1}$)
$h(x)$	workpiece shape
J, $\vec{J}$	electric current density ($A\,cm^{-2}$)
J_a	Jacobian
K_e	electrical conductivity of electrolyte ($\Omega^{-1}\,m^{-1}$)
k	thermal conductivity of electrolyte ($W\,m^{-1}\,K^{-1}$)
m	mass flux rate ($kg\,m^{-2}\,s^{-1}$)
n	unit normal of a surface
P	pressure (Pa)
Pr	Prandtl number
Re	Reynolds number
R_g	gas constant ($J\,kg^{-1}\,K^{-1}$)
$r(x)$	required workpiece shape
s	coordinate along gap (m)
T	electrolyte temperature (K)
u, v	velocity of electrolyte flow ($m\,s^{-1}$)
V_A	velocity of anode dissolution ($m\,s^{-1}$)
V_C	velocity of cathode ($m\,s^{-1}$)
W	energy generation rate ($W\,m^{-2}$)

Greek symbols

α	void fraction
γ	conductance constant, see Equation 7 (K^{-1})
θ	angle (see Fig. 1)
Λ	current efficiency
λ_a	electrochemical equivalent ($g\,C^{-1}$)
μ	viscosity coefficient of electrolyte ($kg\,m^{-1}\,s^{-1}$)
ρ	density ($kg\,m^{-3}$)
τ	shear stresses ($N\,m^{-2}$)
ϕ	electric potential (V)
ϕ_a	applied voltage (V)

Subscripts

0	condition at entrance of electrolyte
a	anode
c	cathode
e	exit condition
f	electrolyte
g	gas phase
i	initial condition

Superscripts

0	dimensionless parameter
k	iteration counter
m	generalization of heterogeneous conduction mechanism, see Equation 7

1. Introduction

Electrochemical machining (ECM) is a process used to shape the anode metal, namely the workpiece, by high-rate electrochemical dissolution. An electric potential is applied across the electrodes. The cathode, namely the tool, is normally moved towards the anode with constant velocity. To carry away the dissolved metal the electrolyte is used to flow between the electrodes. The rate of machining does not depend on the hardness

of the metal and there is no wear on the tool, this machining can thus be used to shape any metal. Recently, ECM had widely been applied in the aeronautics, space, and other high precision industries.

Previously, most researchers have attempted to predict a workpiece shape machined by a given tool. This is called a direct problem. Analytic techniques include the $\cos\theta$ method [1], the analogue method [2] and the complex variables method [3]. Various numerical techniques, including the finite difference method [4, 5] and the finite element method (FEM) [6], have also been applied. But all the above work is limited to consideration of the effect of the electric field only. Either void fraction or temperature of the electrolyte is taken into account in the majority of the papers [7–9]. Thorpe and Zerkle [10, 11] proposed a one-dimensional, two-phase fluid flow model and showed that most ECM can be treated as a quasi-steady process. Jain *et al.* [12] simulated ECM processes in which the metal removal rate is affected by the electric and flow fields. Hourng solved a one-dimensional, bubbly two-phase [13] and a two-dimensional, single-phase [14] flow field to predict the workpiece shape and the variations of electrolyte properties between electrodes.

However, the determination of the tool shape to produce a desired workpiece shape is more practical for the engineering design. Mathematically, it is an inverse problem, which is generally difficult to solve under complex boundary geometry. In recent years several algorithms have been proposed. For example, Das and Mitra used the boundary element method [15], Lacey applied the complex variables method [16], and Hunt developed multigrid techniques [17] and an embedding method [18]. But the effect of the thermal-fluid properties on the tool shape was not considered.

The purpose of the present work, is to consider the inverse problem in ECM without ignoring important effects. The electric potential field is solved by a finite element method to reduce the calculation time, and a body-fitted transformation technique is applied repeatedly to generate the mesh system during the process. A one-dimensional two-phase model and a two-dimensional single-phase model are then used to simulate the flow field during electrochemical machining. The variation of velocity, temperature and void fraction of the electrolyte are demonstrated and analysed in detail. The workpiece shape machined by the predicted tool agrees well with the required workpiece shape. The relative error can be reduced under 0.002. Understanding of the machining conditions and the numerical parameters is helpful in the design of the tool shape.

2. Theoretical model

2.1. *Electric field and variation of interelectrode gap*

A two-dimensional electrochemical machining configuration is sketched in Fig. 1. In steady situations

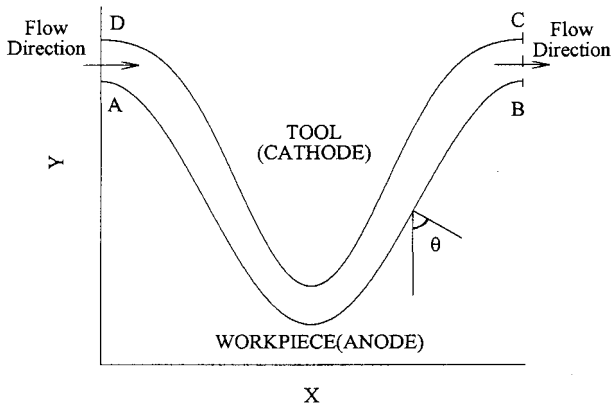

Fig. 1. A typical ECM configuration.

conservation of charge gives $\nabla \cdot \vec{J} = 0$, where $\vec{J}$ is the electric current density. In the gap between the workpiece surface and the tool surface, an electric current flows through the electrolyte with the electric current density $\vec{J} = -K_e \nabla\phi$, where ϕ is the potential and K_e is the electrolyte electrical conductivity. The potential distribution between the electrodes is thus governed by

$$\nabla \cdot (K_e \nabla\phi) = 0 \tag{1}$$

The corresponding boundary conditions, as shown in Fig. 1, are

$$\left.\begin{array}{ll} \text{(i)} & \text{along the anode surface } \overline{\text{AB}}\text{: } \phi = \phi_a \\ \text{(ii)} & \text{along the cathode surface } \overline{\text{DC}}\text{: } \phi = 0 \\ \text{(iii)} & \text{along the flow inlet } \overline{\text{AD}}\text{: } \dfrac{\partial\phi}{\partial \text{n}} = 0 \\ \text{(iv)} & \text{along the flow exit } \overline{\text{BC}}\text{: } \dfrac{\partial\phi}{\partial \text{n}} = 0 \end{array}\right\} \tag{2}$$

where ϕ_a is the applied voltage and 'n' is the unit normal of a surface. The variation of electrode gap g is given by

$$\frac{\partial g}{\partial t} = V_A - V_C \tag{3}$$

where V_C is the local cathode feed velocity and V_A is the dissolution velocity of the anode in the direction normal to the tool surface. By Ohm's law and Faraday's law, Equation 3 can be written as

$$\frac{\partial g}{\partial t} = \frac{\Lambda \lambda_a J}{\rho_a} - f_r \cos\theta \tag{4}$$

where λ_a is the electrochemical equivalent, Λ the current efficiency, ρ_a the anode density and f_r the feed rate of the tool. The equilibrium gap thickness at inlet, g_e, can be represented by [10]

$$g_e = \frac{\Lambda \lambda_a K_e}{\rho_a} \frac{\phi_a}{f_r} \tag{5}$$

The current density normal to the workpiece, J, is

$$J = \left| K_e \frac{\partial\phi}{\partial \text{n}} \right| \tag{6}$$

and the electrolyte conductivity can be represented [10] by

$$K_e = K_{e0}(1-\alpha)^m [1 + \gamma(T - T_0)] \tag{7}$$

where the zero subscript denotes the condition at the entrance of the electrode gap, γ the conductance constant and T the electrolyte temperature. The exponent m represents a generalization of heterogeneous conduction mechanism and is taken to be 1.75 [10]. The void fraction is defined as

$$\alpha = \frac{g_g}{g} \tag{8}$$

where g_g represents the dimension occupied by the gas phase in the gap. For the single-phase two-dimensional model the void fraction is zero and the electrolyte electrical conductivity in Equation 7 reduces to

$$K_e = K_{e0}[1 + \gamma(T - T_0)] \tag{9}$$

2.2. *Thermal and fluid equations*

2.2.1. Bubbly two-phase model (One-dimensional, two-phase model). In electrochemical machining, the electrolyte flow in the interelectrode gap is assumed to be one-dimensional with only one independent space variable, s, along the gap. Since the amount of dissolved metal is small, the flow is assumed to contain only two phases, namely, hydrogen gas and the electrolyte. The electrolyte is assumed to be incompressible while the hydrogen obeys the perfect gas law. The thermal conductivity and heat capacity of hydrogen are small compared to that of the electrolyte; hence, the transport of the thermal energy is dominated by the electrolyte rather than the gas phase. Furthermore, the temperature difference between electrodes and the electrolyte is not large in the practical situation. Thus, the heat flux transferred from electrodes to the electrolyte is negligible. Under these assumptions, the bubbly-two-phase model [11] can be applied, and the transport equations describing the flow can be derived as follows.

The continuity equation for the gas phase is

$$\frac{\partial}{\partial s}(\rho_g A_g V_g) + \frac{\partial}{\partial t}(\rho_g A_g) = \frac{A_g m_g}{g_g} \tag{10}$$

where A_g is the cross-sectional area and m_g is the mass flux of hydrogen gas generated at the interface and entering the gas control volume. The continuity equation for the liquid electrolyte phase is

$$\frac{\partial}{\partial s}(\rho_f A_f V_f) + \frac{\partial}{\partial t}(\rho_f A_f) = \frac{A_f(m_a - m_g)}{g_f} \tag{11}$$

where m_a is the dissolved mass flux of the anode. The momentum equation for the liquid phase is

$$\rho_g g_g\left[\frac{\partial V_g}{\partial t} + \frac{\partial}{\partial s}\left(\frac{V_g^2}{2}\right)\right] + \rho_f g_f\left[\frac{\partial V_f}{\partial t} + \frac{\partial}{\partial s}\left(\frac{V_f^2}{2}\right)\right] = -g\frac{\partial P}{\partial s} - (\tau_a + \tau_c) - m_a V_f - m_g(V_g - V_f) \tag{12}$$

where P is the pressure, τ_a and τ_c are the shear stresses acting on the anode and cathode. The energy equation is

$$V_f\frac{\partial T_f}{\partial s} + \frac{\partial T_f}{\partial t} = \frac{H(T_a - T_f) + W + m_a(h_a - h_f)}{\rho_f g_f C_f} \tag{13}$$

where H is the convective heat transfer coefficient, T_a is the temperature of the anode, h_f and h_g are the enthalpy of the electrolyte and gas, respectively, and C_f represents the specific heat capacity of the electrolyte. The energy generation rate, W, originating from the current through the electrolyte, can be obtained from Joule's law as

$$W = \vec{E}\cdot\vec{J} = K_e\left[\left(\frac{\partial\phi}{\partial x}\right)^2 + \left(\frac{\partial\phi}{\partial y}\right)^2\right] \tag{14}$$

where $\vec{E}$ is the electrical intensity. Finally, the equation of state for the gas phase is

$$P = \rho_g R_g T_f \tag{15}$$

On applying order-of-magnitude analysis, Thorpe and Zerkle [11] found that the transient behaviour of an ECM process is almost governed by the transient term ($\partial g/\partial t$) in the kinematic equation, Equation 4. They also pointed out that the effect of the electrodes on the electrolyte heating is negligible, that is, the term $H(T_a - T_f) + m_a(h_a - h_f)$ on the right hand side of the energy equation, namely Equation 13, is zero. Furthermore, the term $m_a V_f + m_g(V_g - V_f)$ in the momentum equation (i.e., Equation 12) contributes little to the pressure gradient. These terms are thus also neglected here. The initial and boundary conditions required to solve the kinematic and conservation equations include the initial electrode gap $g_i(s)$, the electrolyte velocity at the entrance V_0, the exit pressure P_e, and the electrolyte temperature at the entrance T_0. At the entrance, the void fraction is zero since there is no gas.

2.2.2. One-phase, two-dimensional model. In an ECM with a complex cathode shape, it is necessary to use a two-dimensional model to solve the thermal-fluid field in the interelectrode gap. The flow in the interelectrode gap contains the electrolyte, hydrogen gas and the dissolved metal. Since the amount of hydrogen gas and dissolved metal is small, the momentum and energy transport are determined by the electrolyte. For the convenience of analysis, the flow is thus assumed to be incompressible, laminar and contains only the electrolyte. The continuity and momentum equations of the single-phase, two-dimensional flow can be expressed in rectangular coordinates as

$$\frac{\partial u^0}{\partial x^0} + \frac{\partial v^0}{\partial y^0} = 0 \tag{16a}$$

$$u^0\frac{\partial u^0}{\partial x^0} + v^0\frac{\partial u^0}{\partial y^0} = -\frac{\partial P^0}{\partial x^0} + \frac{1}{Re}\left(\frac{\partial^2 u^0}{\partial x^{0^2}} + \frac{\partial^2 u^0}{\partial y^{0^2}}\right) \tag{16b}$$

and

$$u^0\frac{\partial v^0}{\partial x^0}+v^0\frac{\partial v^0}{\partial y^0}=-\frac{\partial P^0}{\partial y^0}+\frac{1}{Re}\left(\frac{\partial^2 v^0}{\partial x^{0^2}}+\frac{\partial^2 v^0}{\partial y^{0^2}}\right) \quad (16c)$$

where the zero superscript denotes the dimensionless parameter, and Re (the Reynolds number) $=\rho_f u_0 g_e/\mu$, $P^0=(P-P_e)/\rho_f u_0^2$, P_e the exit pressure, and u_0 the velocity at the entrance.

The incompressible Navier–Stokes equations, namely Equations 16(a), (b) and (c) are nonlinear and solved here by the intermediate parameters approach. The procedure and the necessary boundary conditions in solving the flow field are described in Bush and Marshall [19] and Hourng [14], respectively.

Since the electrolyte velocity and the corresponding Echert number are small, the energy dissipation can be neglected. By using the inlet temperature of the electrolyte as the characteristic temperature, the dimensionless form of the energy equation is

$$u^0\frac{\partial T^0}{\partial x^0}+v^0\frac{\partial T^0}{\partial y^0}=\frac{1}{Pr\,Re}\left(\frac{\partial^2 T^0}{\partial x^{0^2}}+\frac{\partial^2 T^0}{\partial y^{0^2}}\right)+W^0 \quad (17)$$

where Pr (the Prandtl number) $=\mu C_f/k$, $W^0=Wg_e/(\rho_f C_f T_0 u_0)$ and W is the energy generation rate as mentioned above. The electrolyte properties, such as thermal conductivity, k, specific heat capacity, C_f, and viscosity coefficient, μ, are assumed to be constants.

In solving the energy equation, the temperature at inlet, workpiece, and tool are specified, while the exit temperature is assumed to be fully developed.

2.3. *Inverse problem analysis*

In the direct problem, even if considering the influence of the thermal-fluid properties, the workpiece shape for a given tool shape can readily be predicted numerically. For this reason, the embedding method that searches among the set of direct solutions for various tools is applied here until a match for the required workpiece shape is found.

As shown in Fig. 1, a_1, a_2,…,a_m are the coefficients of a Fourier cosine series of degree m associated with any given tool shape $f(x)$ and b_1, b_2,…,b_m are the coefficients associated with the workpiece shape $h(x)$ resulting from the direct problem with this given $f(x)$. Finally, c_1, c_2,…,c_m are the coefficients of a Fourier cosine series of degree m associated with the required workpiece shape $r(x)$. If $[A]$ is equivalent to $(a_1, a_2,\ldots, a_m)^T$ with sim ilar expressions applicable to $[B]$ and $[C]$, then the numerical iteration can be written as [18]

$$[A]^{k+1}=[A]^k+[\Delta A]^k \quad (18)$$

and

$$[\Delta A]^k=([C]-[B]^k)\times[J_a]^{-1} \quad (19)$$

where k is the iteration counter and J_a is the Jacobian whose (i, j)th element is represented by

$$\frac{\partial b_i}{\partial a_j}\cong\frac{1}{\varepsilon}\left[b_i(a_1^k,\ldots,a_j^k+\varepsilon,\ldots,a_m^k)-b_i(a_1^k,\ldots,a_j^k,\ldots,a_m^k)\right] \quad (20)$$

where $\varepsilon=10^{-3}$ is used in this paper. For each coefficient b_i of the Fourier cosine series of degree m the direct problem must be solved $(m+1)$ times for $b_i(a_1^k,\ldots,a_j^k,\ldots,a_m^k)$ and every $b_i(a_1^k,\ldots,a_j^k+\varepsilon,\ldots,a_m^k)$, where $j=1, 2,\ldots, m$. Hence, for large m the procedure could be very costly, and we should select a proper size for m.

2.4. *Curve fitting for the workpiece shape*

The workpiece predicted numerically from the direct problem is a set of discrete points but not a function. Therefore, the coefficients of the workpiece shape function $h(x)$ must be obtained by curve fitting. In this paper we approximate $h(x)$ by the Fourier cosine series as

$$h(x)=\sum_{i=0}^{m}b_i\phi_i(x) \quad (21)$$

where $\phi_i(x)=\cos(2i\pi x/L)$, L the length of the electrode in the x-direction. The coefficients of $h(x)$ are determined by the least-squares method, in which the square of the difference between the workpiece shape y and $h(x)$ is

$$\mathrm{ERR}(h)=\sum_{k=1}^{n}[h(x_k)-y_k]^2 \quad (22)$$

Since $\mathrm{ERR}(h)$ is a function of b_i, the coefficients b_i can thus be solved by

$$0=\frac{\partial \mathrm{ERR}(h)}{\partial b_i}=\sum_{k=1}^{n}2[h(x_k)-y_k]\times\frac{\partial}{\partial b_i}[h(x_k)-y_k] \quad (23)$$

that is,

$$\sum_{i=0}^{m}b_i\left[\sum_{k=1}^{n}\phi_i(x_k)\phi_j(x_k)\right]=\sum_{k=1}^{n}[y_k\cdot\phi_j(x_k)] \quad (24)$$

Equation 24 can be written in a matrix form as

$$[D][B]=[F] \quad (25)$$

The elements D_{ji} and F_j are represented by

$$D_{ji}=\sum_{k=1}^{n}[\phi_i(x_k)\phi_j(x_k)] \quad (26)$$

$$F_j=\sum_{k=1}^{n}[y_k\cdot\phi_j(x_k)] \quad (27)$$

3. Numerical procedure

In ECM, the workpiece shape is irregular and changes continuously during the machining process. A

good distribution of nodal points is needed for calculating the electric potential and the fluid field. A body-fitted coordinate transformation technique is applied where a Poisson equation is utilized to transform the irregular physical domain to the rectangular computational domain [20]. A smooth grid distribution is thus generated. The spatial accuracy is of the order of $[(\Delta\xi)^2,(\Delta\eta)^2]$.

In the present paper, the electric potential is solved by the finite element method (FEM) to reduce the CPU time. The thermal-fluid field for the one-dimensional, bubbly two-phase model and the single-phase two-dimensional model are solved by the procedures similar to Hourng [13] and [14], respectively. All the numerical calculations were performed on an IBM320/RS970 workstation, and a typical CPU time required for a direct problem with grid size of 201×15 was about 558 s. The numerical procedure is as follows:

(i) Give the required workpiece shape and the machining conditions.
(ii) Generate mesh distribution by the body-fitted coordinate transformation technique.
(iii) Calculate the distribution of the electric potential.
(iv) Calculate the thermal-fluid properties, and then calculate the electrical conductivity.
(v) Calculate the new shape of the workpiece, and repeat step (ii) to (iv) until the interelectrode gap reaches equilibrium, that is, the relative error at each single node is less than 10^{-4}.
(vi) Calculate the coefficients of the workpiece shape by curve fitting method.
(vii) Use the embedding method to correct the tool shape, and repeat step (ii) to (v) until the corrected term $[\Delta A]$ is less than 10^{-4}.

The tool shape obtained is step (vii) is evaluated by the relative error defined as

$$\mathrm{RERR} = \mathrm{AERR}/g_e \tag{28}$$

and

$$\mathrm{AERR} = \frac{1}{n}\sum_{k=1}^{n}(\Delta y_k)^2 = \frac{1}{n}\sum_{k=1}^{n}[r(x_k) - y_k]^2 \tag{29}$$

where $r(x_k)$ is the required workpiece shape at any single node k as stated above, while y_k is the workpiece shape if machined by the calculated tool shape.

4. Results and discussion

4.1. *Analysis of thermal-fluid flow*

The machining conditions and the electrolyte properties used in the present study are listed as Tables 1 and 2, respectively. As shown in Fig. 2, the numerical predictions by various models are in good qualitative agreement with the experimental data [21]. In particular, the result obtained by the one-dimensional two-phase model is closer to the experimental data than other results obtained by neglecting the flow effects and the two-dimensional single-phase model. Thus the thermal-fluid properties can be properly simulated by the one-dimensional two-phase model to obtain a good prediction in electrochemical machining.

In electrochemical machining, the workpiece shape is affected by the machining conditions. Normally, the equilibrium gap thickness becomes larger as the applied voltage is increased or the feed rate of the tool towards the workpiece is decreased and, accordingly, the difference between the workpiece shape and the tool shape becomes larger. The equilibrium workpiece shapes in various machining conditions are shown in Fig. 3. For each case, the applied voltage and the tool feed rate are different, but their ratio (ϕ_a/f_r) is kept the same. This indicates that the workpiece shapes are almost identical, as their (ϕ_a/f_r) values are the same, except for the region near the exit. The workpiece shape near the exit becomes slightly different from the tool, shape, as the applied voltage is increased. This may be explained by the distributions of the electrolyte temperature and the void fraction as shown in Fig. 4. As the applied voltage is increased, the heat generated by the current in the electrolyte between the electrodes is large; thus the electrolyte temperature becomes higher. The void fraction between the electrodes also becomes larger as the applied voltage is increased. As indicated in Equation 7, the electrolyte conductivity decreases as the electrolyte temperature in reduced or as the void fraction increases. Since the void fraction is dominant in this case, the electrolyte conductivity becomes lower as the applied voltage is increased. Due to the fact that the workpiece removal rate is proportional to the electrolyte conductivity, the gap thickness thus decreases along the flow direction.

Table 1. Working conditions of electrochemical machining

Condition	*Figure number*				
	2	*3*	*5*	*8,10,11*	*9*
Tool feed rate 10^{-6}, f_r/m s^{-1}	9.27		5	9.05	9.05
Applied voltage, ϕ_a/V	19.5		10	20	20
Temperature at entrance, T_0/K	297.5	300	313	297.5	297.5
Electrolyte flow flux 10^{-6}, Q/m^2 s^{-1}	1750	1500	3750	1750	750
Electrochemical equivalent 10^{-5}, λ_a/g C^{-1}			9.3161		
Metal density, ρ_a/kg m^{-3}			2698		
Current efficiency, Λ/%			92.5		

Table 2. Physical properties of the electrolyte ($NaCl + H_2O$)

Electrolyte conductivity, $K_{e0}/\Omega^{-1}\,m^{-1}$	7
Electrolyte density, $\rho_f/kg\,m^{-3}$	1027
Specific heat capacity 10^3, $Crf/J\,kg^{-1}\,K^{-1}$	4.18
Thermal constant, $x\gamma/K^{-1}$	0.016
Viscosity coefficient 10^{-3}, $\mu/kg\,m^{-1}\,s^{-1}$	0.781
Thermal conductivity, $k/W\,m^{-1}\,K^{-1}$	0.63

If the curvature of the electrode shape varies significantly, the electrolyte flow is two-dimensional, and the single-phase, two-dimensional model is needed to simulate the distribution of the thermal-fluid properties. As shown in Fig. 5, where the tool shape is triangular, a recirculation region occurs downstream of the corner. In an actual electrochemical machining process, the hydrogen gas and the heat generated by the current will be trapped in this recirculation region and the local metal removal rate will thus be affected. Consequently, a two-dimensional flow model should be used in the simulation.

4.2. *Tool design by the inverse method*

In the tool design of electrochemical machining by the inverse method, a convergent and rational shape of the tool can be obtained if suitable machining parameters are chosen. For a workpiece shape of the

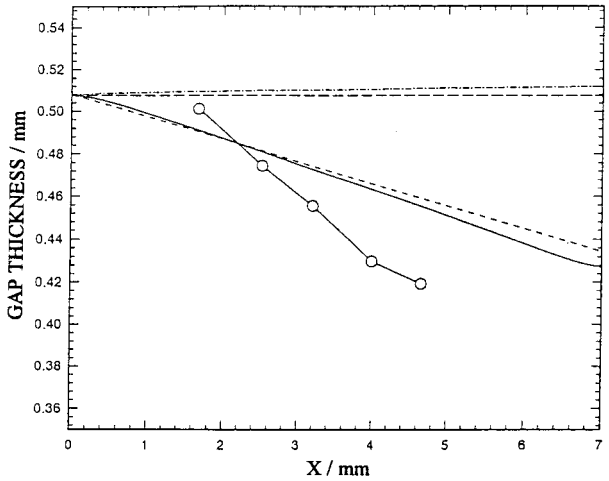

Fig. 2. Comparisons of workpiece shape between numerical and experimental results. Key: (○) experimental data [21]; (- - - - -) Hopenfeld and Cole; (– – –) neglect flow effects model; (——) one-dimensional two-phase model; (·····) two-dimensional single-phase model.

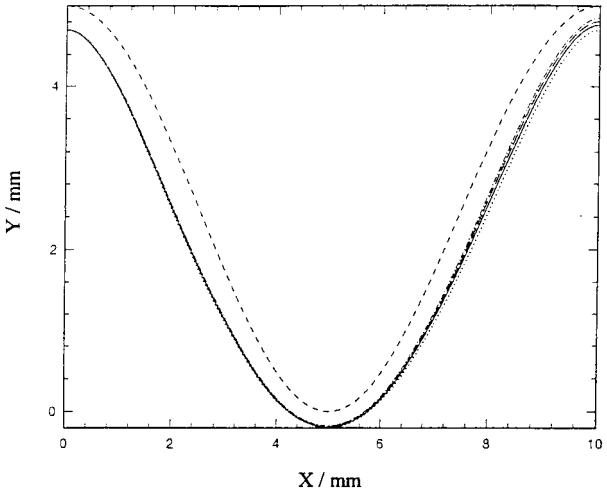

Fig. 3. Workpiece shapes in equilibrium for different applied voltages and cathode feed rates, ratios are the same, (ϕ_a/f_r) 1000 V mm^{-1} s. Tool shape is $2.5 + 2.5\cos(\pi x/5)$. Key: (- - - -) cathode shape; (·····) neglect flow shape; (-·-·-) $\phi_a = 20$ V, $f_r = 2\times10^{-2}$ mm s^{-1}; (– – –) $\phi_a = 10$ V, $f_r = 1\times10^{-2}$ mm s^{-1}; (——) $\phi_a = 5$ V, $f_r = 5\times10^{-3}$ mm s^{-1}.

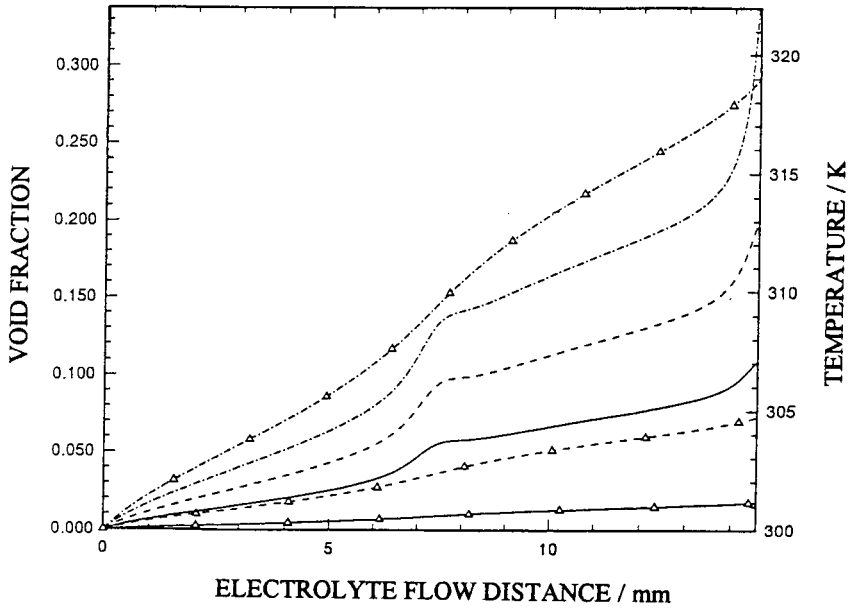

Fig. 4. Variation of void fraction and temperature along stream path for different applied voltages and cathode feed rates, but ratios are the same. Void fraction: (·····) $\phi_a = 20$ V, $f_r = 2\times20^{-2}$ mm s^{-1}; (-----) $\phi_a = 10$ V, $f_r = 1\times10^{-2}$ mm s^{-1}; (——) $\phi_a = 5$ V, $f_r = 5\times10^{-3}$ mm s^{-1}. Temperature: (-·△-·) $\phi_a = 20$ V, $f_r = 2\times10^{-2}$ mm s^{-1}; (- -△- -) $\phi_a = 10$ V, $f_r = 1\times10^{-2}$ mm s^{-1}; (–△–) $\phi_a = 5$ V, $f_r = 5\times10^{-3}$ mm s^{-1}.

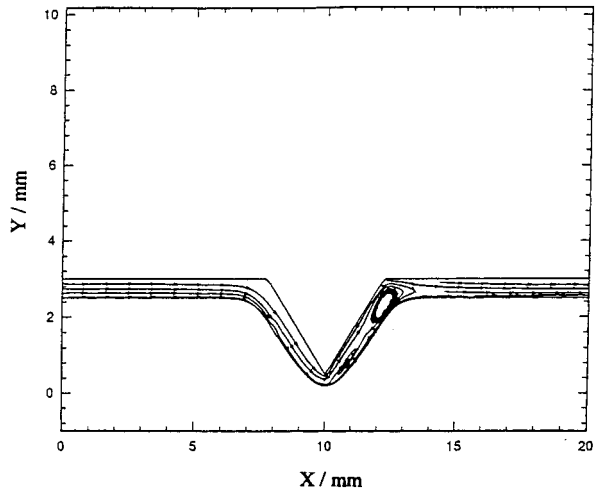

Fig. 5. Streamlines in interelectrode region for the tool shape with a corner.

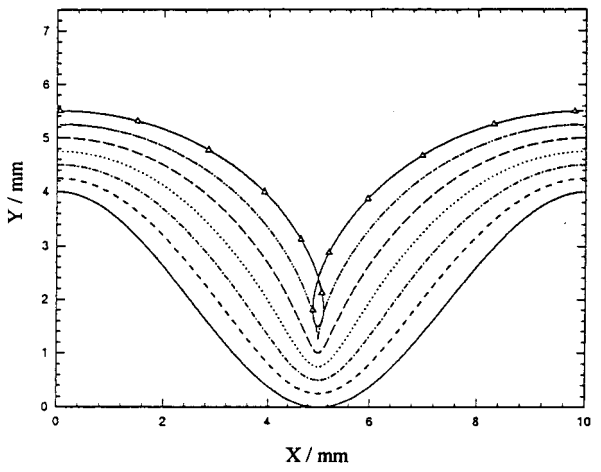

Fig. 7. Desired workpiece shape ($\beta = 2$) and tool shapes predicted by different values of ϕ_a/f_r: (—△—) 6709.02, (·····) 5590.85, (– – –) 4472.68, (——) 3354.51, (·····) 2236.34 and (- - - - -) 1118.17 V mm^{-1} s; (——) desired workpiece.

form $r(x) = \alpha + \beta \cos(2\pi x/L)$ the workpiece will become sharper as β increases. Figure 6 shows a sharp workpiece with $\beta = 5$. If the tool feed rate toward the workpiece is large or the applied voltage is small, such that the ratio (ϕ_a/f_r) is small, then the tool shape obtained by the inverse method is a proper shape. The corresponding equilibrium gap thickness is small, and the difference in shape between the workpiece and tool is small. However, as the ratio (ϕ_a/f_r) increases to 2236.34 V mm^{-1} s such that the equilibrium gap thickness increases to 0.5 mm, a needlepoint tool is needed to produce the desired workpiece. Furthermore, no tool exists to produce the given workpiece if the feed rate is even smaller or the applied voltage is larger. Similar results are obtained for workpiece with $\beta = 2$ as shown in Fig. 7, in which various tools can be used under different machining conditions to produce the given workpiece. Therefore, a high tool feed rate or a low applied voltage is preferred in designing a rational tool to produce a workpiece, especially a sharp workpiece.

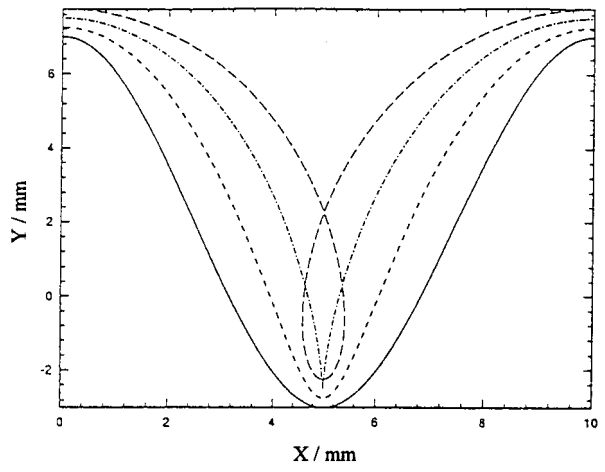

Fig. 6. Desired workpiece shape ($\beta = 5$) and tool shapes predicted by different values of ϕ_a/f_r: (– – –) 3354.51, (·····) 2236.34 and (- - - - - -) 1118.17 V mm^{-1} s; (——) desired workpiece.

After a tool shape is obtained by the inverse method with/without consideration of the thermal-fluid effect, the workpiece produced by the designed tool must be recalculated to compare with the desired workpiece. All these workpieces are calculated with consideration of the thermal-fluid effect in order to be consistent with the actual machining situation. The calculated tool shapes with/without consideration of the flow effect and the resulting workpiece shapes shown in Fig. 8 in which the desired workpiece is of the form $r(x) = 2 + 1.5\cos(\pi x/5)$. The workpiece shape calculated from the tool shape with consideration of the flow effect agrees well with the desired workpiece shape. The relative errors are listed in Table 3. The relative error of the workpiece for the case considering the flow effect in the tool design comes partially from the curve fitting process where a symmetrical cosine function is used to fit a nonsymmetric workpiece shape. The nonsymmetrical workpiece shape is due to the fact that the fluid and thermal properties are not symmetrical in the inlet and exit regions; the metal removal rate is also thus not the same in these regions. Therefore, the relative error increases for the case with low electrolyte flux, in which the thermal-fluid effect is greater. The workpiece calculated by the tool without consideration of flow effects agrees with the desired workpiece shape only in the front region. This is because the thermal-fluid effect becomes stronger as the electrolyte flows further downstream.

As the desired workpiece shape is a cosine function with half period, as shown in Fig. 9, the calculated workpiece shape by tool, with consideration of the flow effect, is coincident with the desired workpiece shape, even when the electrolyte flow is very small (750 mm^2 s^{-1}). This shows that the error from the curve-fitting process is lower for a workpiece of nonsymmetrical shape. However, the workpiece shape calculated form the tool without consideration of the flow effect is very different form the desired workpiece shape.

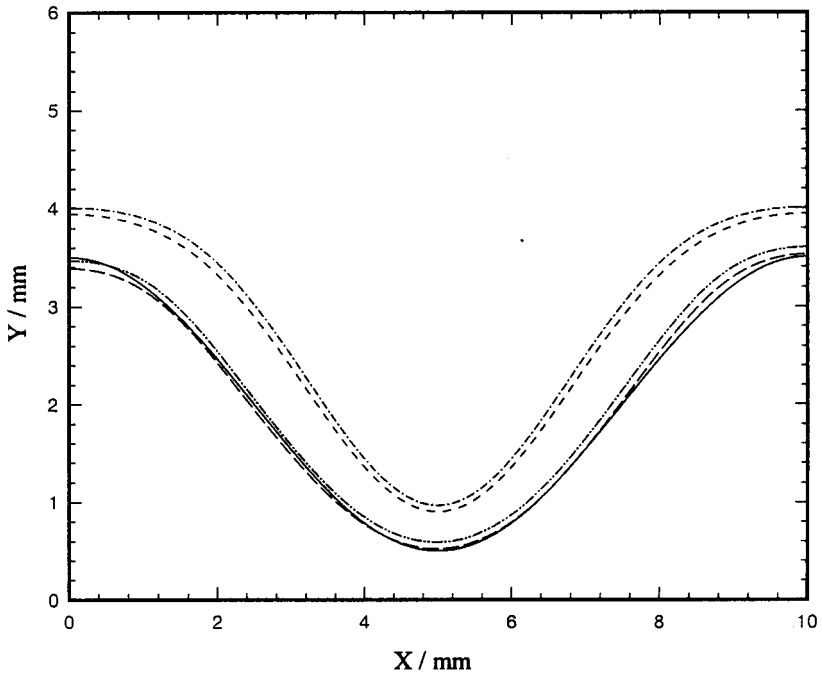

Fig. 8. Predicted tool shapes with/without the flow effect and the corresponding workpiece shapes. Desired workpiece shape is $r(x) = 2 + 1.5\cos(\pi x/5)$. Key: (·····) tool shape neglecting flow effect (tool1); (- - - - -) tool shape considering flow effect (tool2); (·····) workpiece shape obtained from tool1; (– – –) workpiece shape obtained form tool2; (——) desired workpiece shape.

Table 3. Relative errors of the workpiece for various machining conditions

Figure	*With/without considering the thermal-fluid effect in the tool design*	*m*	*Relative error* /%
Fig. 8	yes	3	0.4619
Fig. 8	no	3	0.9350
Fig. 9	yes	3	0.1044
Fig. 9	no	3	1.6437
Fig. 10	yes	3	0.8874
Fig. 10	yes	5	0.7803
Fig. 11	yes	2	1.9983
Fig. 11	yes	3	0.8837
Fig. 11	yes	5	0.2270

In the inverse method, the degree m in the Fourier series taken for the curve fitting of the tool and workpiece is important, especially for a given workpiece with a sharp shape. Figure 10 shows the tools designed and the resulting workpieces with $m = 3$ and $m = 5$, respectively. The calculated workpiece with $m = 5$ is slightly closer to the desired workpiece than the calculated workpiece with $m = 3$. As the desired workpiece is sharp, as shown in Fig. 11, a large m is necessary to give a good result. However, the corresponding calculation time increases as m increases. Therefore, a proper value of m is important to reduce the relative error, as well as the computa-

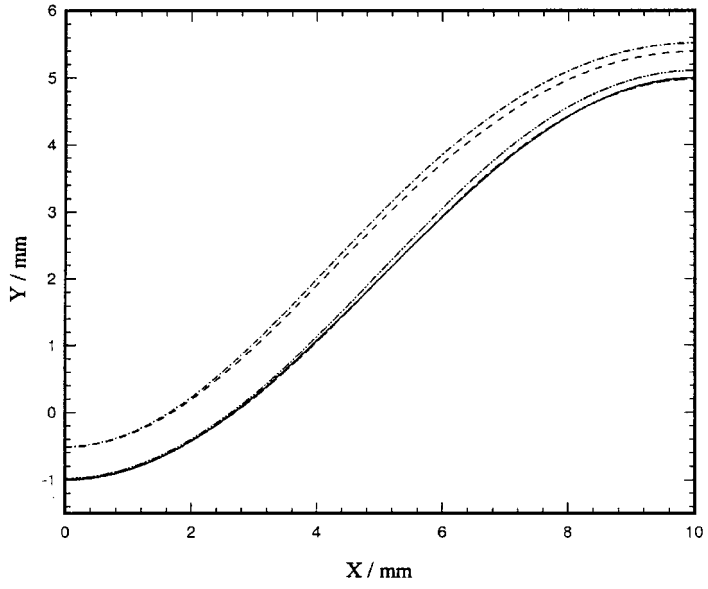

Fig. 9. Predicted tool shapes with/without the flow effect and the corresponding workpiece shapes. Desired workpiece shape is $r(x) = 2 - 3.0\cos(\pi x/10)$. Key: as given in Fig. 8.

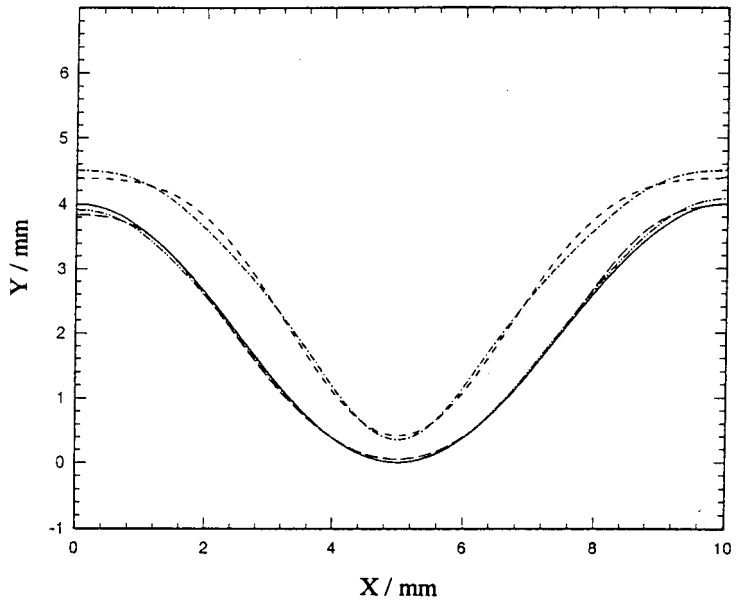

Fig. 10. Predicted tool shapes and corresponding workpiece shapes for various degrees of m in Fourier series. Desired workpiece shape is $r(x) = 2 + 2.0\cos(\pi x/5)$. Key: (- - - - -) tool shape ($m = 3$); (·····) tool shape ($m = 5$); (– – –) workpiece shape ($m = 3$); (·····) workpiece shape ($m = 5$); (——) desired workpiece shape.

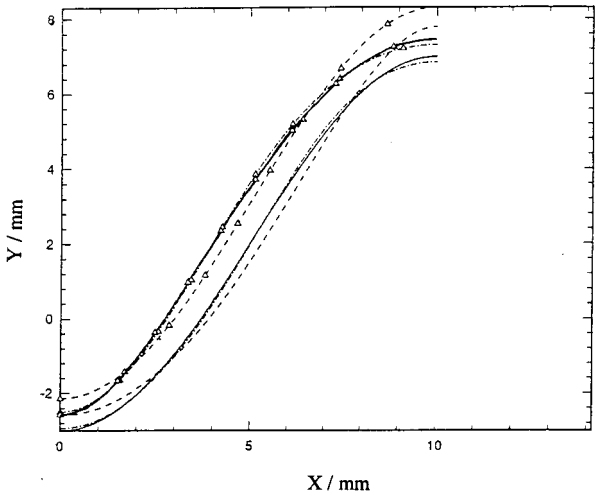

Fig. 11. Predicted tool shapes and corresponding workpiece shapes for various degrees of m in Fourier series. Desired workpiece shape is $r(x) = 2 - 5.0\cos(\pi x/10)$. Key: (- - △ - -) tool shape ($m = 2$); (-·△-·) tool shape ($m = 3$); (–△–) tool shape ($m = 5$); (- - - - -) workpiece shape ($m = 2$); (·····) workpiece shape ($m = 3$); (——) workpiece shape ($m = 5$) (·····) desired workpiece shape.

tion time. In the present case, the relative error can be reduced to about 0.002 if m is taken to be 5.

5. Conclusions

A numerical method is used to predict a tool shape for a required workpiece shape in electrochemical machining. Results show that the relative error of the corresponding workpiece in the present calculations can be reduced to about 0.002 when proper machining conditions and numerical parameters are chosen. The effect of the thermal-fluid properties should be considered in the inverse problem, and the void fraction is the most important factor in determining the electrolyte conductivity. A one-dimensional two-phase model is suitable to simulate the thermal-fluid field if the curvature of the electrodes does not vary sharply. In contrast, a two-dimensional model should be used if the electrodes are sharp.

As the desired workpiece shape becomes sharper, proper machining conditions such as high tool feed rate, low applied voltage and adequate electrolyte flow are preferred to design a tool of appropriate shape. Furthermore, the degree m in the Fourier series taken for the curve fitting of the tool must also be increased to reduce the relative error.

References

[1] A. L. Krylov, *Soviet Phys.* Doklady **13** (1968) 15.
[2] P. Lawrence, Ph. D. Thesis, Leicester University, UK (1997).
[3] D. E. Collett, R. C. Hewson-Brown and D. W. Windle, *J. Eng. Math.* **4** (1970) 29.
[4] V. K Jain and P. C. Pandey, *Precision Eng.* **2** (1980) 195.
[5] M. B. Nanayakkare, Ph. D. Thesis, University of Strathclyde, UK (1977).
[6] V. K. Jain and P. C. Pandey, *Int. J. Mach, Tool Des. Res.* **22** (1982) 341.
[7] H. Tipton, Proceedings of the 5th International Conference on Machine Tool Research, Brimingham, UK, Sept. (1964), p. 509.
[8] K. Kawafune, T. Mikoshiba, K. Noto and K. Hirata, *CIRP Ann.* **15** (1967) 65/1–65/13.
[9] F. Hopenfeld and R. R. Cole, *J. Eng. Indust., ASME Trans.* **88** (1966) 455.
[10] J. F. Thorpe and R. D. Zerkle, *Int. J. Math. Tool Des. and Res.* **9** (1969) 131.
[11] J. F. Thorpe and R. D. Zerkle, 'Fundamentals of Electrochemical Machining', edited by C. L. Faust (Princeton, NJ, 1971), p. 1.
[12] V. K. Jain, P. G. Yogindra and S. Murugan, *Int. J. Mach. Tools Manufact.* **27**(1) (1987) 113.
[13] L. W. Hourng and C. S. Chang, *J. Appl. Electrochem.* **23** (1983) 316.

[14] L. W. Hourng and C. S. Chang, *J. Appl. Electrochem.* **24** (1994) 1170.
[15] S. Das and A. K. Mitra, *Int. J. Num. Methods Eng.* **35** (1992) 1045.
[16] A. A. Lacey, *J. Inst. Math. Appl.* **34** (1985) 259.
[17] R. Hunt, *J. Comp. Phys.* **65** (1986) 448.
[18] R. Hunt, *Int. J. Num. Methods Eng.* **29** (1990) 1177.
[19] A. W. Bush and G. S. Marshall, 'Flow Modelling in Industrial Processes' (Ellis Horwood, 1989), p. 164.
[20] J. P. Thompson, F. C. Thames and C. W. Mastin, *J. Comput. Phys.* **24** (1977) 274.
[21] J. Hopenfeld and R. R. Cole, *J. Eng. Indust.* Aug. (1969) 755.